IJEMD-M, 4 (1) (2026) https://doi.org/ 10.54938/ijemdm.2026.04.1.600

International Journal of Emerging Multidisciplinaries:

Mathematics

Research Paper

Journal Homepage: www.ojs.ijemd.com

ISSN (print): 2790-1998

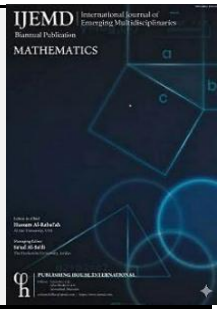

Analysis of MHD-Squeezed Darcy-Forchheimer Nanofluid Flow Between *h*-Distance Horizontal Plates by Computing Approach

Yasir Iqbal [1], Farheen Kanwal [1], Huma Tayyab [1]*, Kainat Waheed [2], Qazi Mahmood Ul-Hassan [1]

1. Department of Mathematics, University of Wah, Pakistan.

2. Department of Mathematics, COMSATS University Islamabad, Pakistan.

ABSTRACT

This study investigates magnetohydrodynamic (MHD) compressed Darcy-Forchheimer nanofluid flow between two parallel plates separated by a distance h and over a nonlinear stretching sheet. The study examines porosity, friction, and a consistently applied magnetic field perpendicular to the lower plate, utilizing the Darcy-Forchheimer porous medium to facilitate horizontal axis flow. We investigate the movement of heat and mass through the examination of Brownian diffusion and thermophoresis. By employing appropriate similarity transformations, the system's highly nonlinear partial differential equations are transformed into ordinary differential equations. Hybrid computational methods have been developed by combining the fourth-order Adams-Bashforth numerical method with artificial neural networks optimized using the Levenberg-Marquardt algorithm. These empirical data sets provide the foundation for an artificial neural network model. With both traditional and modern computational techniques available, predictions of parameter combinations for a particular system may be quickly updated. Increased fluid viscosity reduces the rate of movement. However, the combined forces of thermal diffusion and thermophoresis elevate the temperature in the surrounding fluid layer due to thermal gradients and increased surface area.

Keywords: Artificial Intelligence (AI); Magnetohydrodynamic (MHD); Nanomaterial; Adams Numerical solver.

Email Addresses : iyasir663@gmail.com (Yasir Iqbal) , farheenkanwal032@gmail.com (Farheen Kanwal) , humaq807@gmail.com (Huma Tayyab) , kainatwaheed031@gmail.com (Kainat Waheed) , qazimahmood@uow.edu.pk (Qazi Mehmood-ul-Hassan)

1. Introduction:

By looking carefully and thinking critically, we can understand how nature's physical, chemical and biological processes interact with each other. Science identifies the fundamental laws of how things work by looking carefully, conducting well-controlled experiments & thinking clearly about results. Scientists build mathematical models that predict outcomes in disciplines such as physics, biology, engineering and economics. These models allow scientists to understand how complex real world systems function in much greater detail. These models become more accurate, reliable & useful in solving both engineering problems and improving the way companies operate as advancements are made within the field of science. Fluid Mechanics, Heat Transfer and Mass Transfer deal with the individual processes that can be studied independently in many physical systems. These processes include the movement of materials confined between two flat surfaces, the movement of materials over stretching surfaces and material movement going through cylindrical tunnels. Squeezing flow is one area of study which has significant application in numerous disciplines. The squeezing flow is defined as when two moving surfaces contact each other or separate from each other thereby causing fluids to flow between them. The idea of squeezing flow is useful in many areas of engineering including but not limited to chemical manufacturing, food processing and mechanical/biochemical engineering [1]. This information will continue to be studied throughout the various engineering disciplines.[2] started the first study of squeezing flow in the late 1800s. His work set the stage for ideas that are still used in research today.

Nanofluids are widely used in different industries including semiconductor production, automotive cooling systems, power generation facilities, and healthcare applications globally. These fluids demonstrate remarkable attributes, including thermal stability, distinctive optical properties, and enhanced electromagnetic responses. The integration of nanofluids composed of minuscule particles can mitigate some challenges. Choi innovated the notion, illustrating that traditional thermal liquid refrigerants might be theoretically improved substantially [3]. These refrigerants generally demonstrate low thermal conductivity [4]. This constraint has fostered new opportunities for innovation and creativity in heat regulation applications.

[5] examined on of entropy generation in the flow of squeezed nanofluids between parallel plates, considering slip effects. [6] conducted a thermodynamic analysis of three-dimensional magnetohydrodynamic squeezed flow with changing characteristics. [7] investigated the importance of nanoparticle radius and inter-particle distance in constrained nanofluid flow. [8] conducted an examination of entropy generation in magnetohydrodynamic blood flow through a porous compressed tube containing magnetic particles. [9] conducted a computer analysis of the squeezing flow of nanofluids in rotating channels. [10] reported observations on the Darcy-Forchheimer flow of water-based carbon nanotubes between two rotating disks with homogeneous-heterogeneous reactions.

Nanofluids, consisting of base fluids including suspended nanoparticles, offer a compelling method to markedly improve thermal transfer in liquid cooling systems. Methanol and oil are two frequently utilized base liquids. [11] examined the unsteady flow of a squeezing nanofluid between two parallel plates, incorporating a first-order chemical reaction and velocity slip. [12] presented a regression analysis of the flow of squeezing-induced hybrid nanofluid in a Darcy-Forchheimer porous media. Heat exchangers regulate the rate of heat transfer, and electronic cooling can improve the efficiency of various processes. The thermal relaxation time parameter is utilized to characterize and regulate the cooling duration of

heated surfaces. [13] conducted a computational analysis on the squeezed flow of modified hybrid nanofluid, incorporating thermal radiation and Cattaneo-Christov heat flux. [14] investigated the magnetohydrodynamic squeezed flow of Jeffrey nanofluid between two parallel disks, incorporating heat radiation. [15] examined the bioconvective Couette-Poiseuille flow of pseudoplastic nanofluid within a parallel microchannel under Robin boundary conditions. [16] conducted a numerical analysis of entropy creation in Darcy-Forchheimer flow of hybrid nanofluid, incorporating thermal radiation and heat generating effects. These investigations examine shortcomings in Fourier's law of heat conduction within particular real-world scenarios. The heat flow model is based on the concept of energy through the parabolic differential equation, which reflects initial energy perturbations caused by either magnetic or thermal influences on the fluid system's boundary conditions. This study presents the above problems using a complete computer-assisted modelling (involving conventional numerical methodology and modern artificial intelligence techniques). The mathematical formulation defines a viscous, incompressible, magnetohydrodynamic nanofluid constrained between two parallel plates separated by a distance h, with flow passing through a Darcy-Forchheimer porous medium. We use the NDSolve function in Mathematica software to numerically solve the governing partial differential equations, which we then convert into dimensionless ordinary differential equations using the right similarity transformations. This gives us a complete dataset that includes a wide range of parameter combinations.

An important emerging artificial intelligence approach is called artificial neural networks (ANNs). On the base of information that travels over the network through learning, either inside or outwardly, ANNs are an evolutionary adaptive system in a number of situations. A collection of connections (weights) that give a depiction that works well with the training set are created as part of the learning process. In order to address a variety of differential equation-based problems, the problematic numerical results are largely developed by modelling ANNs and optimizing them by combining non-linear and methods of linear exploration. Modern developments in stochastic numeric computer solvers offer non-linear models of corneal aspect [17], non-linear astrophysical systems [18,19], and mathematical models based on delay differential equation [20], financial model [21], dust density model [22], plasma physics [23], nonlinear Emden-Fowler equation [24], singular differential model [25], bioinformatics [26], atomic physics [27], fluid dynamics issues [28,29], electromagnetic [30], heat conduction [31], and ground motion prediction model [32].

A dataset of numerically derived sources will be used to develop training datasets for Artificial Neural Network (ANN) models, in conjunction with implementations of ANN architectures designed to use the Levenberg-Marquardt Algorithm as an optimization technique. The hybrid marketplace approach combines the physical accuracy of numerical solutions, and the predictive and computational advantages of machine learning techniques to enable rapid and accurate parameter optimization and real-time engineering prediction capabilities for numerous practical engineering applications.

The Introduction section has been substantially improved to provide a more comprehensive background of the considered physical and computational model. Additional details have been incorporated to clearly motivate the study, particularly emphasizing the role of magnetohydrodynamic (MHD) effects, porous media flow, Darcy–Forchheimer dynamics, and hybrid/tri-hybrid nanofluid systems in advanced thermal transport applications.

Furthermore, the literature review has been significantly expanded to include recent and relevant studies on nanofluid flow modeling, heat transfer enhancement mechanisms, and machine learning–based simulation approaches. Special attention has been given to Levenberg–Marquardt based artificial neural networks (LMS-ANN) and their successful application in solving nonlinear transport phenomena.

Recent advancements in hybrid and ternary nanofluids, along with their thermal performance in complex geometries and under electromagnetic effects, have been critically discussed. The gap in existing literature has been clearly identified, particularly the lack of integrated studies combining MHD Darcy–Forchheimer flow with intelligent computational frameworks.

Novelty:

This research describes a new way of using was part of a new hybrid computational method. This research has developed realistic models for predicting how non-Newtonian nanofluids will transfer heat using the Adams numerical method to produce Data files that have been optimized by using ANN and the Levenberg-Marquardt training algorithm and as results, represents a pioneering achievement in Computational Nanofluid Dynamics through integrating Traditional Numerical Methods with Advanced Artificial Intelligence techniques to allow Engineers to optimize as many parameters as desired quickly and in real time, making this development a key contribution to industry and engineering, and greatly improves our understanding of the basic physics of complex flow via Computational Nanofluid Dynamics.

2. Mathematical Model Transformation:

By utilizing similarity transformations, the nonlinear partial differential equations (PDEs) that govern the MHD nanofluid movement through a Darcy-Forchheimer porous medium in a squeeze configuration are converted into a set of ordinary differential equations (ODEs). Therefore, the required computational effort to solve the PDEs can be reduced without losing any physical principles governing the interaction between the magnetic field and porous medium resistance and the effects of applied squeeze flow. Through the systematic variation of governing parameters such as Magnetic Parameter, Viscosity Parameter, Porosity Parameter, Forchheimer Number, Brownian Motion Parameter, Thermophoresis Parameter, Schmidt Number, and Chemical Reaction Parameter, a complete reference data set for the MHD-Darcy-Forchheimer Nanofluid Model will be produced for the different operational conditions using the NDSolve function of the Mathematica software. This extensive dataset enables detailed investigation of parameter interactions and their combined effects on velocity, temperature, and concentration characteristics in squeezed flow through porous media.

Consider about a steady, incompressible, two-dimensional magnetohydrodynamic nanofluid flow between two horizontal parallel plates that are h apart. The coordinate system is set up so that the lower plate is at $y = 0$ and the upper plate is at $y = h$. The lower plate is stretched at a speed of $u = zx_1$, where z is a positive constant that shows how fast it is stretching and x_1 is the coordinate along the stretching direction. A magnetic field of strength B_0 is applied to the lower plate in the positive y-direction, making it perpendicular to the plate. Figure 1 shows the geometry of considered problem.

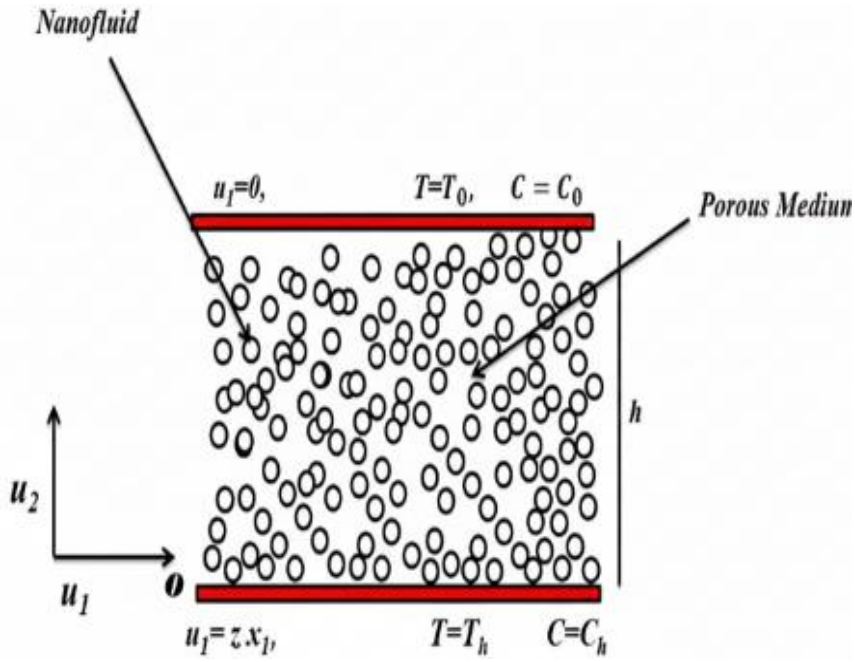

Figure 1: (Geometry of MHD Darcy Forchhimer)

Using the previously given assumptions the continuity, momentum and energy equation are derived as follows.

$$\frac{\partial u_1}{\partial x_1}+\frac{\partial u_2}{\partial x_2}=0, \tag{1}$$

$$u_1\frac{\partial u_1}{\partial x_1}+u_2\frac{\partial u_1}{\partial x_2}=-\frac{1}{P_f}\frac{\partial P}{\partial x_1}+V\left(\frac{\partial^2 u_1}{\partial x_1^2}+\frac{\partial^2 u_1}{\partial x_2^2}\right)\frac{-\sigma B_0^2}{P_f}u_1-\frac{v}{k}u_1-Fu_1^2, \tag{2}$$

$$u_1\frac{\partial u_2}{\partial x_1}+u_2\frac{\partial u_2}{\partial x_2}=-\frac{1}{P_f}\frac{\partial P}{\partial x_2}+V\left(\frac{\partial^2 u_2}{\partial x_1^2}+\frac{\partial^2 u_2}{\partial x_2^2}\right) \tag{3}$$

$$u_1\frac{\partial T}{\partial x_1}+u_2\frac{\partial T}{\partial x_2}=\alpha\left(\frac{\partial^2 T}{\partial x_2^2}+\frac{\partial^2 T}{\partial x_1^2}\right)+\tau\left[D_B\left(\frac{\partial C}{\partial x_2}\frac{\partial T}{\partial x_2}+\frac{\partial C}{\partial x_1}\frac{\partial T}{\partial x_1}\right)+\frac{D_T}{T_h}\left(\frac{\partial T}{\partial x_1}\right)^2+\left(\frac{\partial T}{\partial x_2}\right)^2\right], \tag{4}$$

$$\mathrm{u_1}\frac{\partial \mathrm{T}}{\partial \mathrm{x_1}}+\mathrm{u_2}\frac{\partial \mathrm{T}}{\partial \mathrm{x_2}}=\mathrm{D_B}\left(\frac{\partial^2 \mathrm{C}}{\partial \mathrm{x_1^2}}+\frac{\partial^2 \mathrm{C}}{\partial \mathrm{x_2^2}}\right)+\frac{\mathrm{D_T}}{\mathrm{T_0}}\left(\frac{\partial^2 \mathrm{T}}{\partial \mathrm{x_2^2}}+\frac{\partial^2 \mathrm{T}}{\partial \mathrm{x_1^2}}\right), \tag{5}$$

With BCs

$$u_1=u_w=zx_1, u_2=0, C=C_h, T=T_h, \text{ at } x_2=0, \tag{6}$$

$$u_1=0, C=C_0, T=T_0, \text{ at } x_2=h. \tag{7}$$

Differentiation of equation (2) w.r.t. x_2 and equation (3) w.r.t. x_1 and subtraction yield the following combined momentum equation:

$$\frac{\partial u_1}{\partial x_1}\frac{\partial u_1}{\partial x_2}+u_1\frac{\partial^2 u_1}{\partial x_1\partial x_2}+\frac{\partial u_1}{\partial x_2}\frac{\partial u_2}{\partial x_2}+u_2\frac{\partial^2 u_1}{\partial x_2^2}-u_1\frac{\partial^2 u_2}{\partial x_1^2}-\frac{\partial u_1}{\partial x_1}\frac{\partial u_2}{\partial x_1}-u_2\frac{\partial^2 u_2}{\partial x_1\partial x_2}-\frac{\partial u_2}{\partial x_1}\frac{\partial u_2}{\partial x_2}=V\left(\frac{\partial^3 u_1}{\partial x_1^2\partial x_2}+\frac{\partial^3 u_1}{\partial x_2^3}-\frac{\partial^3 u_2}{\partial x_1^3}-\frac{\partial^3 u_2}{\partial x_1\partial x_2^2}\right)\frac{-\sigma B_0^2}{P_f}\frac{\partial u_1}{\partial x_2}-\frac{v}{k}\frac{\partial u_1}{\partial x_2}-2F\frac{\partial u_1}{\partial x_2} \quad (8)$$

Define,

$$u_1=zx_1\frac{\partial f}{\partial eta},u_2=-zhf,(T_0-T_h)\theta(\eta)=(T-T_h),(C_0-C_h)\phi(\eta)=(C-C_h),\eta=\frac{y}{h}. \quad (9)$$

Using (9) in (1), (4), (5), and (8), we have

The transformed ODEs are

$$f^{IV}-P\left(f'f''-ff'''\right)-\lambda M(f'')-f''-2F_r\,(f'f'')=0 \quad (10)$$

$$\theta''+N_b\phi'\theta'+PP_rf\theta'+N_t\theta'^2=0, \quad (11)$$

$$\phi''(\eta)+Pscf(\eta)\phi'(\eta)+\frac{Nt}{Nb}\theta'^{(\eta)}=0 \quad (12)$$

With conditions

$$\begin{aligned} &f'=1,f=0,\theta=1=\phi, \text{ at } \eta=0,\\ &f'=0,f=0,\theta=0=\phi, \text{ at } \eta=1, \end{aligned} \quad (13)$$

3. Analysis of Method

3.1. Adams Numerical Method:

The Adams numerical method, often implemented in software like Mathematica using functions like NDSolve, is a family of numerical methods for solving ordinary differential equations (ODEs). While they are commonly used for initial value problems (IVPs), they can also be adapted for boundary value problems (BVPs). One common approach to solving BVPs using Adams methods is to reformulate the BVP as an IVP and use the shooting method. The two main types are Adams-Bashforth methods (explicit) and Adams-Moulton methods (implicit).

3.2. Adams-Bashforth Methods:

These are explicit methods, meaning they directly calculate the solution at the next time step using information from previous time steps. They are based on interpolating polynomials to approximate the derivative at each step. Commonly used Adams-Bashforth methods include the second-order, third-order, and fourth-order methods.

The general formula for Adams-Bashforth is:

$$y_{\{n+1\}}=\ y_n+\ h\,\Sigma_{\{i=0\}}^{\{k-1\}b}f\left(t_{\{n-i\}},y_{\{n-i\}}\right), \quad (14)$$

Here, h is the step size, b are the coefficients based on polynomial interpolation, f is the function representing the derivative dy/dt.

Test Problem:

Consider for an example the problem:

$$y' = f(t,y) = 2y, y(0) = 1.$$

The exact solution is $y(t) = e^{\{2t\}}$.

Adams-Bashforth is a four-step method:

$$y_{\{n+4\}} = y_{\{n+3\}} + \left(\frac{h}{24}\right)[55f\left(t_{\{n+3\}}, y_{\{n+3\}}\right) - 59f\left(t_{\{n+2\}}, y_{\{n+2\}}\right) + 37f\left(t_{\{n+1\}}, y_{\{n+1\}}\right) - 9f(t_n, y_n)] \quad (15)$$

We need $y\{n+1\}$, y{n+2}, and y{n+3} to compute the next value y{n+4}. However, the initial values given by $y_0 = 1$. One possibility to resolve this issue is to use the y_1, y_2, y_3 computed by Euler's method as the starting values. For y_1, we use a simple numerical method is Euler's method:

$$y_{\{n+1\}} = y_n + hf(t_n, y_n) \quad (16)$$

Euler's method can be viewed as an explicit multistep method for the degenerate case of one step. This method, applied with step size h = 0.2 on the problem y' = 2y, gives the following results:

$$y_1 = y_0 + hf(t_0, y_0) = 1 + (0.2)(2)(1) = 1.4 \quad (17)$$

$$y_2 = y_1 + hf(t_1, y_1) = 1.4 + (0.2)(2)(1.4) = 1.4 + 0.56 = 1.96 \quad (18)$$

$$y_3 = y_2 + hf(t_2, y_2) = 1.96 + (0.2)(2)(1.96) = 1.96 + 0.784 = 2.744 \quad (19)$$

Now we can use the Adams-Bashforth 4-step method. At t = t_4 = 0.8:

$$y_4 = y_3 + \left(\frac{h}{24}\right)[55f(t_3, y_3) - 59f(t_2, y_2) + 37f(t_1, y_1) - 9f(t_0, y_0)],$$

Since $f(t,y) = 2y$:

$$y_4 = 2.744 + \left(\frac{0.2}{24}\right)[55(2)(2.744) - 59(2)(1.96) + 37(2)(1.4) - 9(2)(1)]$$

$$y_4 = 2.744 + \left(\frac{0.2}{24}\right)[302.84 - 231.28 + 103.6 - 18]$$

$$y_4 = 2.744 + \left(\frac{0.2}{24}\right)[157.16]$$

$$y_4 = 2.744 + 1.3097 = 4.0537 \quad (20)$$

The exact solution at $t = t_4 = 0.8$ *is* $e^{\{2(0.8)\}} = e^{\{1.6\}} = 4.9530$.

The relative error is: $\frac{|4.9530 - 4.0537|}{4.9530} \times 100\% = 18.16\%$

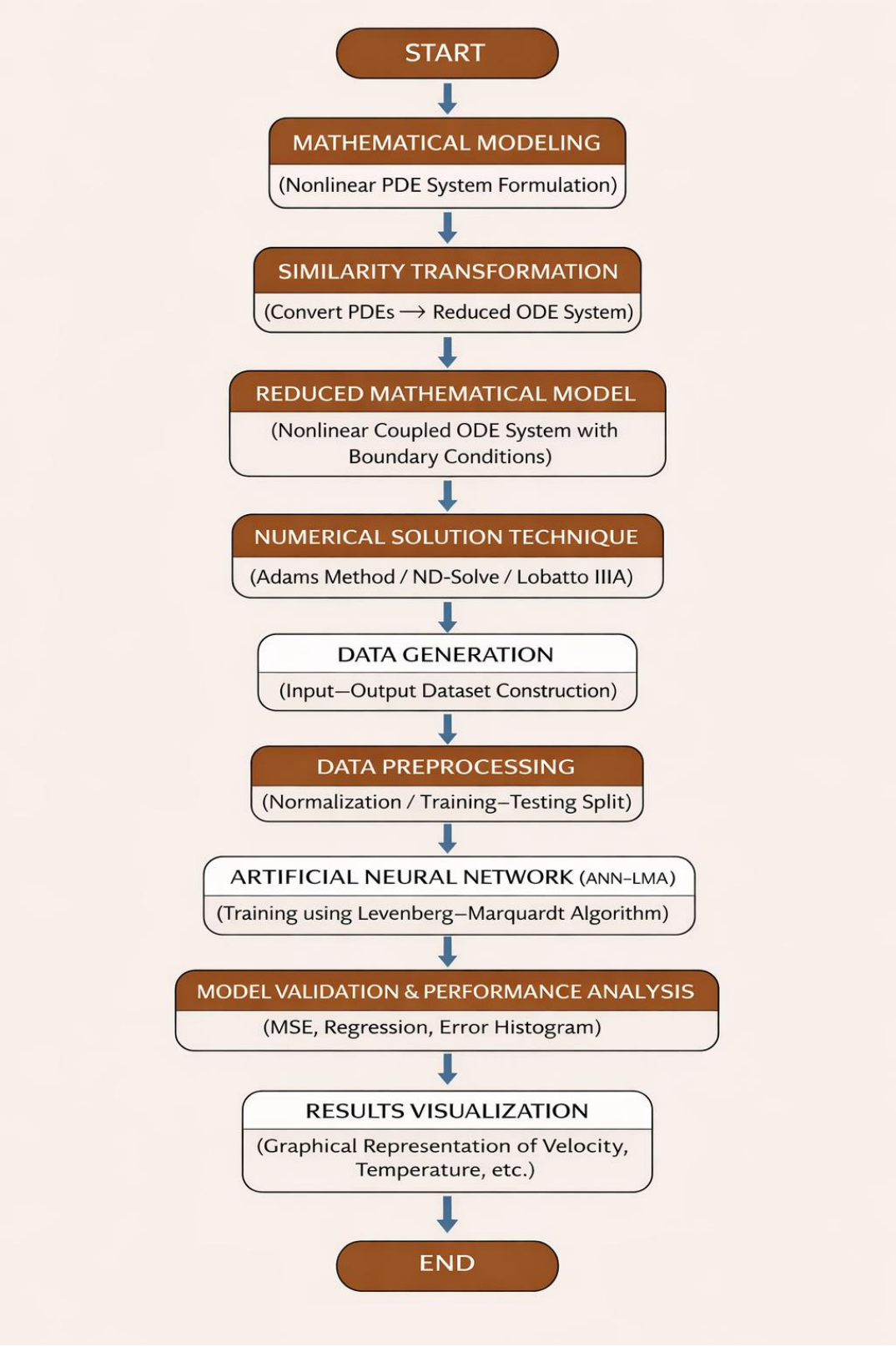

Figure 2. Flow chart

Figure 2 describe the flow chart of study.

3.4. Contribution and Innovative Insight:

The following key contributions and innovations distinguish the present investigation from existing literature:

AI-Driven Numerical Computing Approach:

A numerical computing technique using Artificial Neural Networks (ANNs) that combines Artificial Intelligence (AI) and Machine Learning (ML) has been developed for assessing the MHD Squeezed Darcy-Forchheimer flows. This development represents the very first complete integration of ML methods into this unique flow mechanism, which includes applications with porous substrates or media at two separated distances. The AI method is capable of quickly carrying out parametric sensitivity-analysis and optimizing the dynamical oscillatory patterns of highly complex multiphysics-related problems.

4. Solution Methodology

The NDSolve method is used to numerically solve the set of differential equations, producing input-output pairs for several versions with a step size of. Four different situations are created in order to investigate how different parameter affects flow behaviour. The dataset created for these four scenarios is used to train artificial neural network (ANN) Matlab, as shown in Table 1.

Table 1

Physical Quantities					
Scenarios	**Cases**	**M**	**P**	**Fr**	**Nt**
01	**1**	1	1	1	1
	2	3	1	1	1
	3	5	1	1	1
	4	7	1	1	1
02	**1**	1	1	1	1
	2	1	3	1	1
	3	1	5	1	1
	4	1	8	1	1
03	**1**	0.5	1	0.1	1
	2	0.5	1	2.0	1
	3	0.5	1	5.0	1
	4	0.5	1	10.0	1
04	**1**	1	1	1	0.1
	2	1	1	1	0.3
	3	1	1	1	0.5
	4	1	1	1	0.7

Table 2: ANNs Outcomes

Scenarios	Performance	Training	Gradient	Mu
M	5.8246E-09	1.2E-07	9.9048E-08	1E-09
p	2.1617E-09	2.2E-09	9.9048E-08	1E-09
Fr	1.3053E-07	1.6E-08	9.9048E-08	1E-09
Nt	2.1226E-08	7.7E-09	9.9048E-08	1E-09

4.1 Artificial Neural Networks:

ANNs are computer models based on how the brain is built and how it works. An ANN is a network of "neurons," or nodes that are connected to each other and arranged in different layers.

Input Layer: Gets the raw data or signals from outside.

Hidden Layers: One or more layers where the real work gets done. Through a method called backpropagation, these layers change "weights" to find complex patterns**.**

Output Layer: Makes the final guess or classification.

The Accuracy metric is the main way to measure how well an ANN works. It shows the percentage of correct predictions out of all the test cases that were looked at. Accuracy is a basic way to measure how well a model works, but it might not be enough to give a full picture of how reliable and effective a model is. The main goal of training a neural network is to find the right balance between how complex the model is and how well it can apply what it has learned to new situations. This balance makes sure that the model works well on new data that it hasn't seen before and keeps it from two big problems: underfitting, which happens when the model doesn't capture the underlying patterns in the training data well enough, and overfitting, which happens when the model remembers the training examples too well and can't use what it has learned on new examples. Finding this delicate balance is important for making neural network models that are strong and reliable.

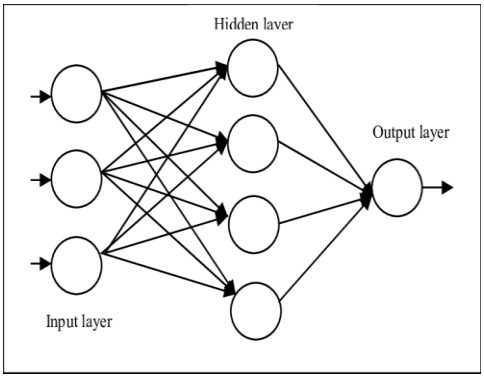

Figure 3: Structure of ANN

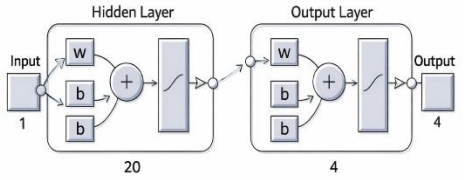

Figure 4: Artificial neural network Diagram

5. Result and Discussion:

The architecture of artificial neural networks (ANNs) is modelled after that of brain .Usually they are made up of hundreds of basic processing units connected in a intricate network of communications. The MHD-Darcy Fr model is solved with a two-step ANN with ODEs. Fig 3 shows the structure of ANN's whereas Fig 4 shows the graphical form of problem. Initial step is to solve ODEs by using NDSolve in Mathematica to calculate velocity, temperature and concentration of various scenarios. The specified model framework allows for the variation of physical parameters. Based on the parameter modification listed in table 1, the scenarios are divided into four types.

The findings and performance of the ANN trained using dataset influenced by the following important factors are presented in this section: the thermo-physical parameter (Nt), the magnetic parameter ,the Forchheimer parameter (Fr) and viscosity parameter P are particularly displayed in figs 5 to 8.

The curve for M are shown in figure5 .The curve for p are displayed in fig.6 and the curve for Fr are shown in fig 7. The curve for Nt are displayed in fig 8. This result demonstrates the value of ANNs in this study.

Fig 5(a),depict the performance graph with Scenarios 1 with Epochs 137 and validation performance is 5.8246E-09.The training state graphs shown in 5(b) with gradient 9.9048E-08.the Error histogram is shown in fig 5(c)and regression in (d)and fit is shown in (e.). Fig 6(a),depict the performance graph with Scenarios 2 with Epochs 137 and validation performance is 2.1617E-09.The training state graphs shown in 6(b) with gradient 9.9048E-08.The Error histogram is shown in fig 6(c)and regression in (d)and fit is shown in (e.). Fig 7(a),depict the performance graph with Scenarios 3 with Epochs 137 and validation performance is1.3053E-07 .The training state graphs shown in 7(b) with gradient 9.9048E-08.the Error histogram is shown in fig 7(c)and regression in (d)and fit is shown in (e.). Fig 8(a),depict the performance graph with Scenarios 4 with Epochs 137 and validation performance is2.1226E-08.The training state graphs shown in 8(b) with gradient 9.9048E-08.the Error histogram is shown in fig 8(c)and regression in (d)and fit is shown in (e.)

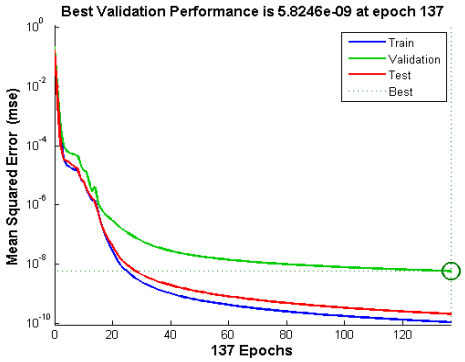

(a) Performance for scenario 1

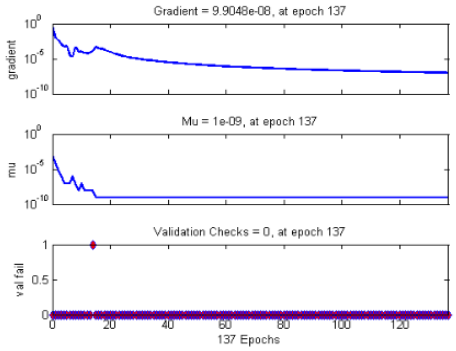

(b) Training state for scenario 1

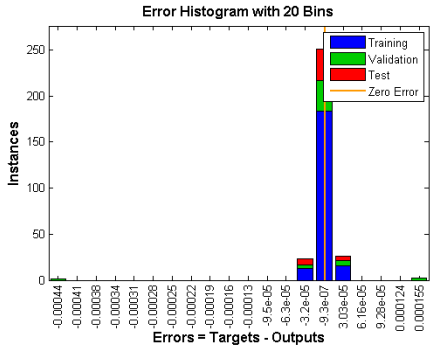

(c) Error Histogram for scenario 1

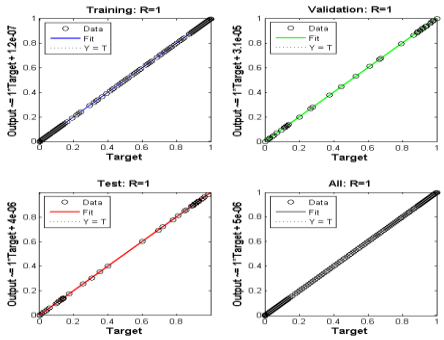

(d) Regression for scenario 1

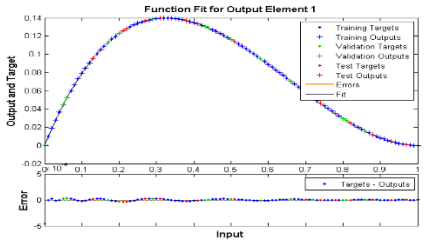

(e) Fitness plot for scenario 1

The plot of ANN that was built to solve M in MHD Darcy-Forchiemer are displayed in Figure 5

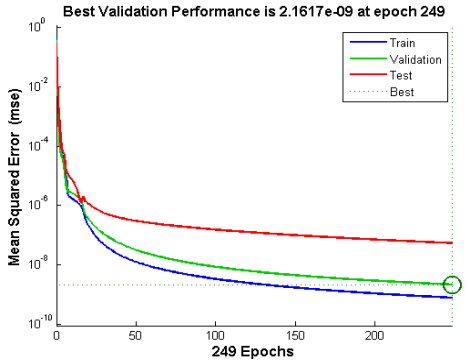

(a) Performance for scenario 2

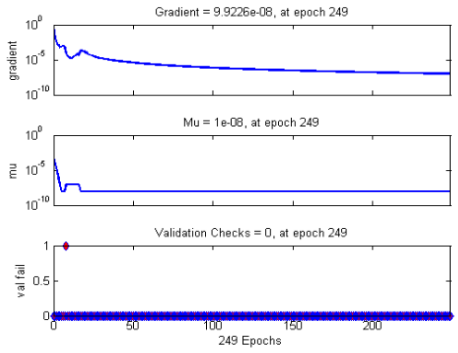

(b) Training state for scenario 2

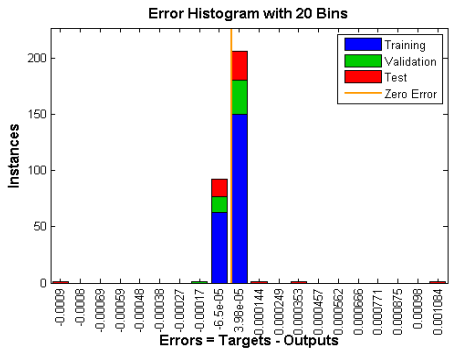

(c) Error Histogram for scenario 2

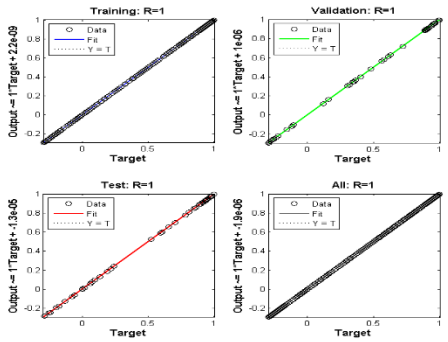

(d) Regression for scenario 2

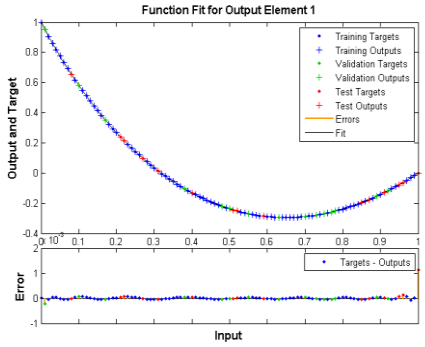

(e) Fitness plot for scenario 2

The plot of ANN that was built to solve p in MHD are displayed in Figure 6

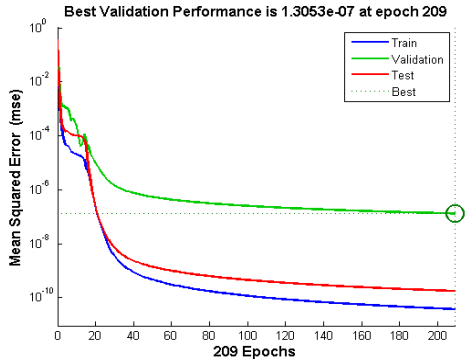

(a) Performance for scenario 3

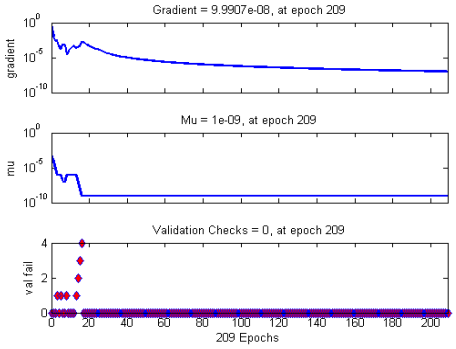

(b) Training state for scenario 2

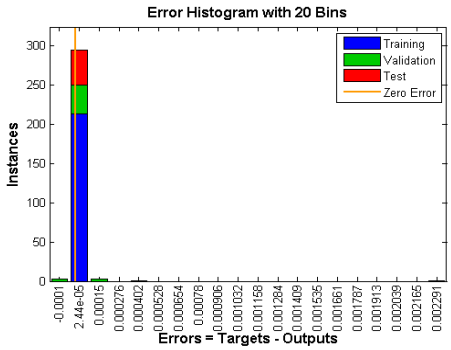

(c) Error Histogram for scenario 3

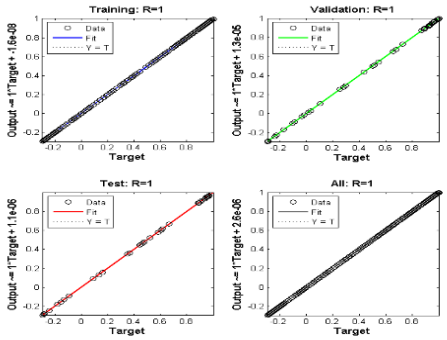

(d) Regression for scenario 3

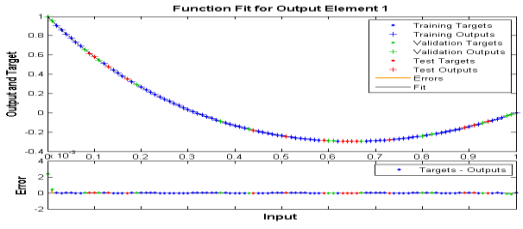

(e) Fitness plot for scenario 3

The plot of ANN that was built to solve Fr in MHD are displayed in Figure 7

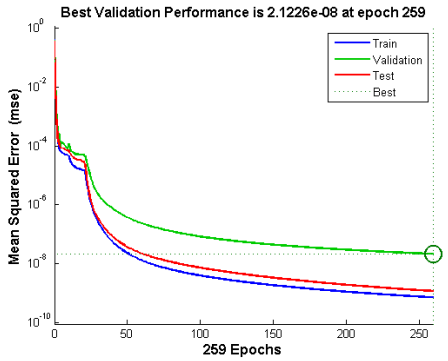

(a) Performance for scenario 4

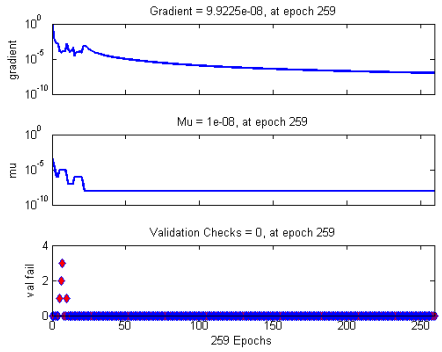

(b) Training state for scenario 4

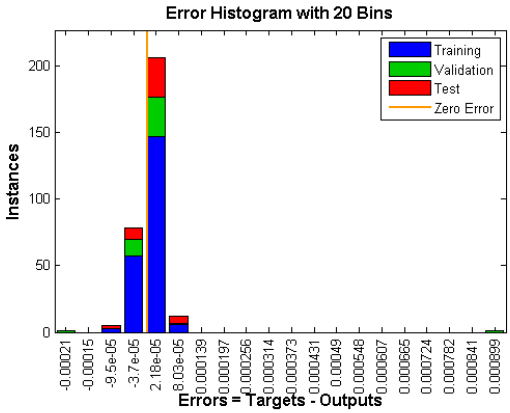

(c) Error Histogram for scenario 4

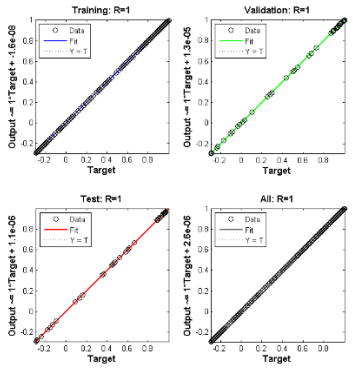

(d) Regression for scenario 4

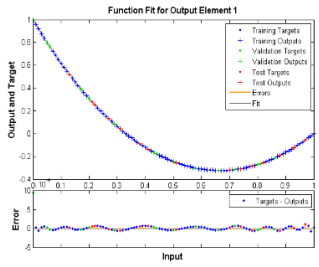

(e) Fitness plot for scenario 4

The Plot of ANN that was built to solve Nt in MHD are displayed in Figure 8

Impact of parameters on Velocity and temperature profile:

The impact of the magnetic field parameter M on the fluid flow through Darcy medium is demonstrated in Figure 9 and 10. These Figures show the variation of profiles $f(\eta)\ and\ f'(\eta)$ for different magnetic field strengths. The results indicates that the magnetic parameter has an inverse relationship with the velocity field. As the magnetic parameter M increases, both velocity profiles experience noticeable decline. The physical explanation for this phenomenon lies in the interaction between the electrically conducting nanofluid and the applied magnetic field. When a uniform magnetic field is applied normal to the lower plate, it induces a Lorentz force that acts perpendicular to both magnetic field direction and flow direction.

The consequences of viscosity parameter P on the velocity profile $f(\eta)\ and\ f'(\eta)$ on figure 13 and 14. The result clearly demonstrate that the larger values of P, there is a consistent decline in the velocity field throughout the flow domain. Physcially , this behavior can be explained by examining the inverse relationship between the viscosity parameter and kinematic viscosity. Figure 3.13 show that the impact of viscosity parameter P on the thermal distribution $\theta(\eta)$. The higher values of P correspond to increased dynamic viscosity of the nanofluid.

Figure 2 and 3 show that the consequences of Forchheimer parameter (Fr) on the velocity profiles $f(\eta)\ and\ f'(\eta)$.A closer examination reveals that the velocity field shows significant reduction for larger values of the Forchheimer. The influence of Brownian motion parameter (Nb) on the concentration distribution $\emptyset'(\eta)$ is depicted in figure 12.
Figure 13 illustrates the consequences of thermophoresis parameter (Nt) on the concentration profile $\emptyset'(\eta)$.

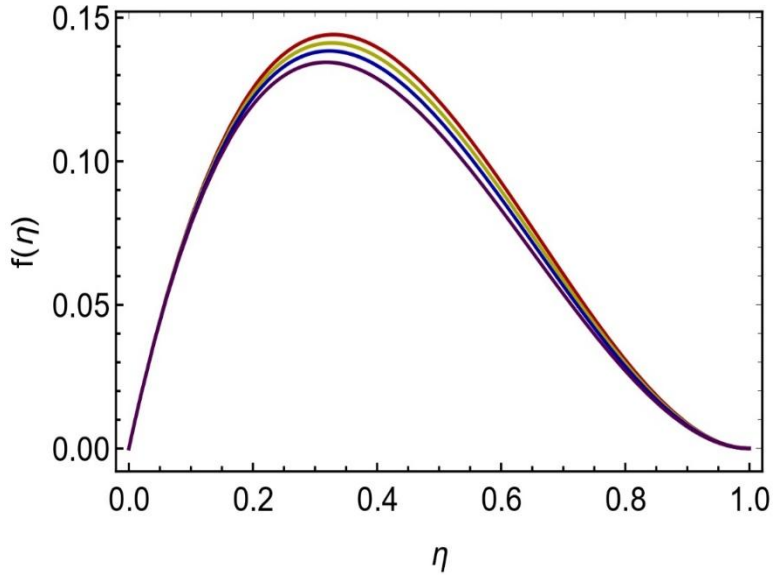

Figure 9

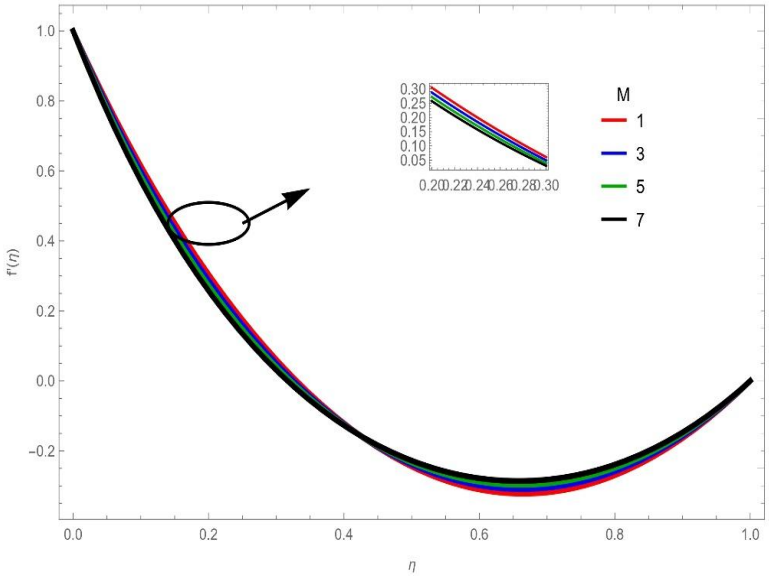

Figure 10

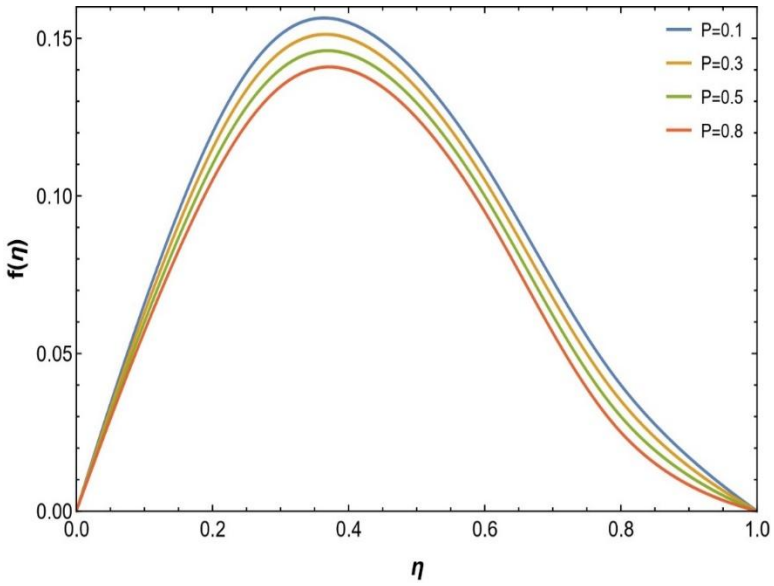

Figure 11

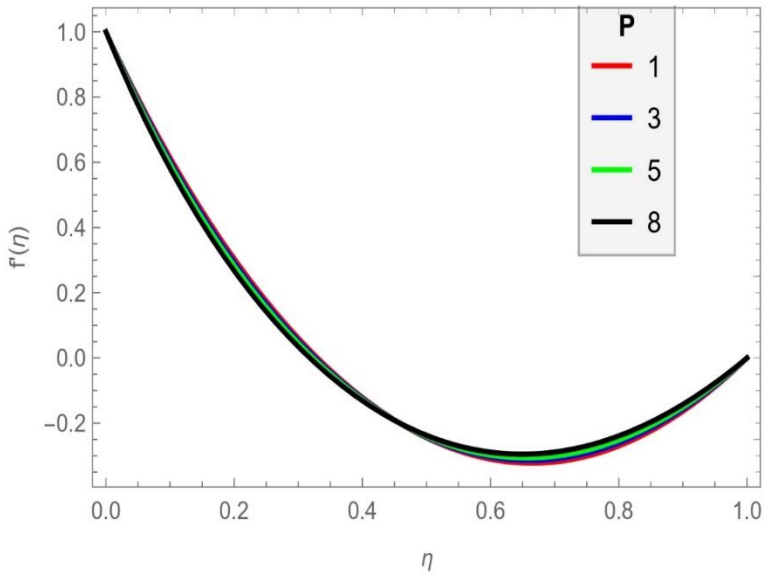

Figure 12

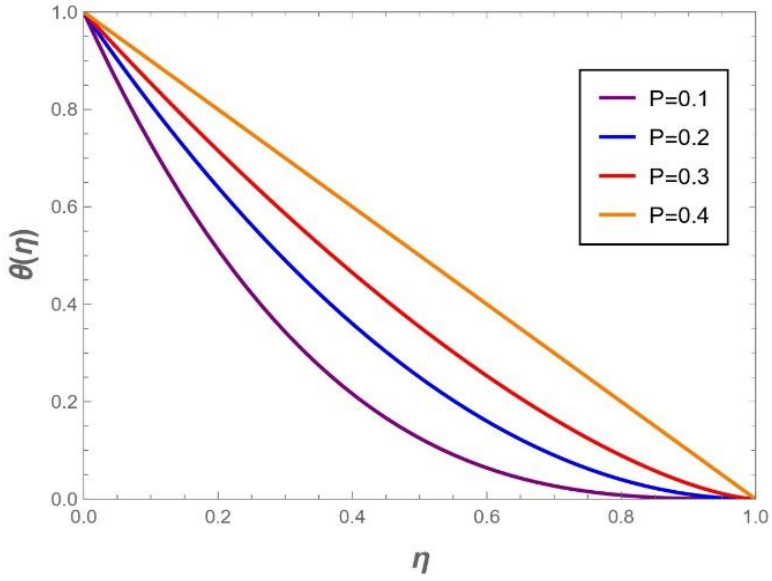

Figure 13

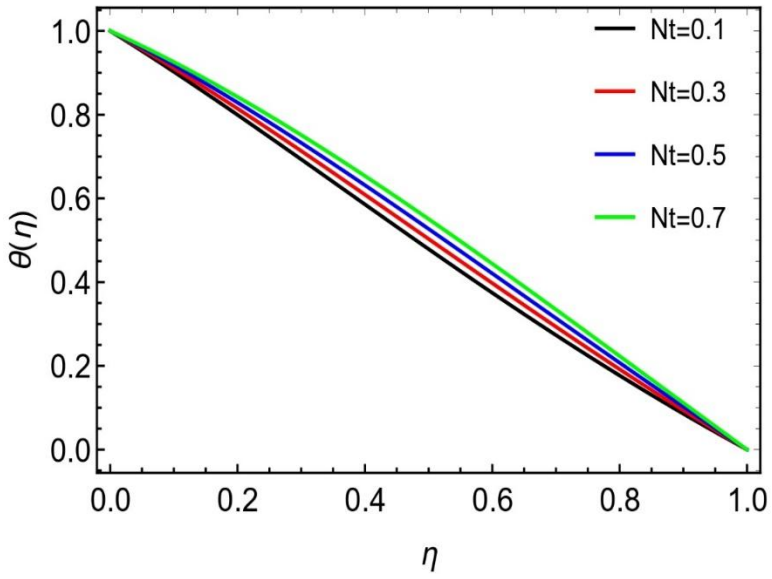

Figure 14

The key findings are :

- As the Forchheimer parameter (Fr) increases, the velocity field $f(\eta)\ and\ f'(\eta)$ decline significantly. The force caused by drag related to flow in porous media causes a drag force to act (extra friction) on the fluid and slow motion of the fluids through the plates. The temperature profile (θ(η)) will rise with increasing magnetic field parameter [M]. The Lorentz force will also increase so velocity profiles will decrease as a result of attraction of opposing magnetic fields acting perpendicular to flow direction.
- The viscosity parameter P has inverse relationships on both velocity and temperature profiles; increasing value of P produces increasing dynamic viscosity which increases internal fluid to fluid friction (viscous) as well as reduce convective heat transfer.
- The parameters of Brownian motion Nb and thermophoresis Nt act to enhance thermal profile properties. The random movement of nanoparticles will increase as the force of thermophoresis increases, and therefore will transfer more rapidly from regions of high temperature to areas of low temperature. For the concentration profile Brownian diffusion causes reduction due to enhanced particle dispersion while thermophoresis causes linear enhancement due to directional particle migration along temperature gradients.
- The Nusselt number (heat transfer) reduces for both viscosity parameter and thermophoresis effect. The thermal boundary layer thickens with increasing P and Nt leading to decreased wall temperature gradients.

This study demonstrates the benefits of combining numerical method to address challenging fluid flow issues it can be used partially in system that involves heat transfer over porous medium with magnetic field control.

Outcomes of Study:

This study shows that while Brownian diffusion and thermophoresis greatly improve the temperature distribution within the fluid due to higher thermal gradients and more effective surface interaction, increasing fluid viscosity significantly decreases flow velocity. Building on previous discoveries, the study examines magnetohydrodynamic (MHD) Darcy–Forchheimer nanofluid flow over a nonlinear stretching sheet and between two parallel plates spaced h apart. Important physical factors are included, such as friction, porosity, and a consistent transverse magnetic field. Brownian motion and thermophoretic mechanisms are used to evaluate heat and mass movement. The controlling nonlinear partial differential equations are converted to ordinary differential equations by applying the proper similarity transformations. A hybrid computational framework is developed by integrating the fourth-order Adams–Bashforth method with artificial neural networks optimized via the Levenberg–Marquardt algorithm (ANN-LM). The resulting model demonstrates high accuracy and efficiency, enabling rapid prediction of system behavior under varying parameter conditions.

6. Conclusions:

A thorough numerical analysis of the magnetic hydrodynamic squeezed Darcy-Forchheimer nanofluid flow between tw0h-distance apart horizontal plates is presented in this work. Similarity transformations were used to transform the governing nonlinear partial differential equations (PDEs) into a system of nonlinear ordinary differential equations(ODEs), which were then numerically solved using ND Solve and also in ANN method.

Overall, the work examines the flow of nanofluids under Darcy-Forchheimer equations of parallel plate movement on a nonlinear stretching sheet with porosity, magnetism, and dynamics of nanoparticles. A hybrid study method incorporating Adams-Bashforth method and Levenberg-Marquardt based artificial neural networks are used to efficiently solve the governing equations so as to make precise predictions. The findings suggest that an increase in viscosity decreases the velocity of fluids, whereas Brownian diffusion and thermophoresis improves temperature distribution. On the whole, the suggested model is a legitimate and efficient approach to investigate sophisticated nanofluid flow and heat transfer in porous media.

References:

[1] S.Y. Hann., Y. Kang., H. Cui, and L.G., Zhang, Microgels: from synthesis to tissue regeneration applications. *Biofabrication*, *17*(3), 2025, p.032008.

[2] M.Chandaragi, J. Shetty., R. Choudhari, H. Vaidya, and K.V., Prasad,. Understanding the complex and multifaceted dynamics of squeezing flow: a comprehensive review: M. Chandaragi et al. *Journal of Thermal Analysis and Calorimetry*, , 2025, pp.1-38.

[3] S. U. S. Choi and J. A. Eastman, "Enhancing thermal conductivity of fluids with nanoparticles," in *ASME International Mechanical Engineering Congress and Exposition*, vol. 66, San Francisco, CA: American Society of Mechanical Engineers, 1995, pp. 99-105.

[4] L. Zhang, M. M. Bhatti, and E. E. Michaelides, "Thermodynamic analysis of three-dimensional MHD squeezed flow with variable properties," *Journal of Thermal Analysis and Calorimetry*, vol. 147, no. 11, 2022, pp. 6473-6485.

[5] R. Kumar, G. S. Seth, and A. Bhattacharyya, "Entropy generation analysis of squeezed nanofluid flow between parallel plates with slip effects," *International Journal of Thermal Sciences*, vol. 172, 2022, Article 107315.

[6] L. Zhang, M. M. Bhatti, and E. E. Michaelides, "Thermodynamic analysis of three-dimensional MHD squeezed flow with variable properties," *Journal of Thermal Analysis and Calorimetry*, vol. 147, no. 11, 2022, pp. 6473-6485.

[7] B. Ali, I. Siddique, A. Shafiq, and S. Abdal, "Significance of nanoparticle radius and inter-particle spacing in squeezed nanofluid flow," *Waves in Random and Complex Media*, 2023, doi: 10.1080/17455030.2023.2178847.

[8] B. K. Sharma, R. Gandhi, and M. M. Bhatti, "Entropy generation analysis for MHD blood flow through a porous squeezed channel with magnetic particles," *Colloids and Surfaces A: Physicochemical and Engineering Aspects*, vol. 655, 2022, Article 130259.

[9] K. Ahmed and Q. M. U. Hassan, "Squeezing flow of nanofluids in rotating channels: A computational study," *Numerical Heat Transfer, Part A: Applications*, vol. 83, no. 8, 2023, pp. 915-932.

[10] G. Rasool, A. M. Saeed, A. I. Lare, A. Abderrahmane, K. Guedri, H. Vaidya, and R. Marzouki, "Darcy-Forchheimer flow of water-based carbon nanotubes between two spinning disks with homogeneous-heterogeneous reactions," *Symmetry*, vol. 14, no. 7, 2022, Article 1375.

[11] S. Maiti, S. Shaw, and G. C. Shit, "Squeezing unsteady nanofluid flow among two parallel plates with first-order chemical reaction and velocity slip," *Heat Transfer*, vol. 53, no. 5, 2024, pp. 2431-2456.

[12] K. Muhammad and M. Sarfraz, "Regression analysis of squeezing-induced hybrid nanofluid flow in Darcy-Forchheimer porous medium," *Applied Mathematics and Mechanics*, vol. 46, 2025, pp. 193-208.

[13] K. Muhammad, K. A. M. Alharbi, N. Fatima, and A. Alhowaity, "Squeezed flow of MHNF (modified hybrid nanofluid) with thermal radiation and CC (Cattaneo-Christov) heat flux: A numerical study via FDM," *Materials Science and Engineering: B*, vol. 289, 2023, Article 116268.

[14] K. U. Rehman, W. Shatanawi, and K. Abodayeh, "Magnetohydrodynamic squeezed flow of Jeffrey nanofluid between two parallel disks with thermal radiation," *Frontiers in Energy Research*, vol. 10, 2022, Article 1047656.

[15] M. I. Khan, S. A. Khan, T. Hayat, M. Qayyum, and A. Alsaedi, "Bioconvective Couette-Poiseuille flow of pseudoplastic nanofluid in a parallel microchannel with Robin boundary conditions," *Journal of Molecular Liquids*, vol. 362, 2022, Article 119642.

[16] H. Waqas, M. Fida, D. Liu, U. Manzoor, T. Muhammad, and M. K. Pasha, "Numerical study of entropy generation in Darcy-Forchheimer flow of hybrid nanofluid with thermal radiation and heat generation effects," *Case Studies in Thermal Engineering*, vol. 45, 2023, Article 102990.

[17] I. Ahmad, M. A. Z. Raja, H. Ramos, M. Bilal, and M. Shoaib. Integrated neuro-evolution-based computing solver for dynamics of nonlinear corneal shape model numerically. Neural Computing and Applications, 33:5753–5769, 2021.

[18] I. Ahmad, M. A. Z. Raja, M. Bilal, and F. Ashraf. Bio-inspired computational heuristics to study laneemden systems arising in astrophysics model. SpringerPlus, 5:1–23, 2016.

[19] Z. Sabir, H. A. Wahab, M. Umar, M. G. Sakar, and M. A. Z. Raja. Novel design of morlet wavelet neural network for solving second order lane–emden equation. Mathematics and Computers in Simulation, 172:1–14, 2020.

[20] I. Khan, M. A. Z. Raja, M. Shoaib, P. Kumam, H. Alrabaiah, Z. Shah, and S. Islam. Design of neural network with levenberg-marquardt and bayesian regularization backpropagation for solving pantograph delay differential equations. IEEE Access, 8:137918–137933, 2020.

[21] A. H. Bukhari, M. A. Z. Raja, M. Sulaiman, S. Islam, M. Shoaib, and P. Kumam. Fractional neuro-sequential arfima-lstm for financial market forecasting. Ieee Access, 8:71326–71338, 2020.

[22] I. Jadoon, M. A. Z. Raja, M. Junaid, A. Ahmed, A. ur Rehman, and M. Shoaib. Design of evolutionary optimized finite difference based numerical computing for dust density model of nonlinear van-der pol mathieus oscillatory systems. Mathematics and Computers in Simulation, 181:444–470, 2021.

[23] A. H. Bukhari, M. Sulaiman, M. A. Z. Raja, S. Islam, M. Shoaib, and P. Kumam. Design of a hybrid nar-rbfs neural network for nonlinear dusty plasma system. Alexandria Engineering Journal, 59(5):3325–3345, 2020.

[24] Z. Sabir, M. A. Z. Raja, J. L. Guirao, and M. Shoaib. Integrated intelligent computing with neuro-swarming solver for multi-singular fourth-order nonlinear emden–fowler equation. Computational and Applied Mathematics, 39:1–18, 2020.

[25] Z. Sabir, D. Baleanu, M. Shoaib, and M. A. Z. Raja. Design of stochastic numerical solver for the solution of singular three-point second-order boundary value problems. Neural Computing and Applications, 33:2427– 2443, 2021.

[26] F. Faisal, M. Shoaib, M. A. Z. Raja, et al. A new heuristic computational solver for nonlinear singular thomas–fermi system using evolutionary optimized cubic splines. The European Physical Journal Plus, 135(1):55, 2020.

[27] A. Imran, R. Akhtar, Z. Zhiyu, M. Shoaib, and M. A. Zahoor Raja. Mhd and heat transfer analyses of a fluid flow through scraped surface heat exchanger by analytical solver. AIP Advances, 9(7):075201, 2019.

[28] M. Umar, Z. Sabir, M. A. Z. Raja, M. Shoaib, M. Gupta, and Y. G. S´anchez. A stochastic intelligent computing with neuro-evolution heuristics for nonlinear sitr system of novel covid-19 dynamics. Symmetry, 12(10):1628, 2020.

[29] W. Waseem, M. Sulaiman, S. Islam, P. Kumam, R. Nawaz, M. A. Z. Raja, M. Farooq, and M. Shoaib. A study of changes in temperature profile of porous fin model using cuckoo search algorithm. Alexandria Engineering Journal, 59(1):11–24, 2020.

[30] T. N. Cheema, M. A. Z. Raja, I. Ahmad, S. Naz, H. Ilyas, and M. Shoaib. Intelligent computing with levenberg–marquardt artificial neural networks for nonlinear system of covid-19 epidemic model for future generation disease control. The European Physical Journal Plus, 135:1–35, 2020.

[31] M. A. Z. Raja, M. Umar, Z. Sabir, J. A. Khan, and D. Baleanu. A new stochastic computing paradigm for the dynamics of nonlinear singular heat conduction model of the human head. The European Physical Journal Plus, 133:1–21, 2018.

[32] S. Hammal, N. Bourahla, and N. Laouami. Neural-network based prediction of inelastic response spectra. Civil Engineering Journal, 6(6):1124–1135, 2020.